Available online at www.sciencedirect.com
ScienceDirect
Journal of the European Ceramic Society 27 (2007) 2069–2076
www.elsevier.com/locate/jeurceramsoc

Improved strength-impairing contact damage resistance of $Ti_3Si(Al)C_2$/SiC composites

Detian Wan [a,b], Yanchun Zhou [a,*], Chunfeng Hu [a,b], Yiwang Bao [a]

[a] *Shenyang National Laboratory for Materials Science, Institute of Metal Research, Chinese Academy of Sciences, Shenyang 110016, PR China*
[b] *Graduate School of Chinese Academy of Sciences, Beijing 100039, PR China*

Received 6 April 2006; received in revised form 3 July 2006; accepted 15 July 2006
Available online 11 September 2006

Abstract

The resistance of $Ti_3Si(Al)C_2$-based materials to strength-impairing contact damage was investigated using the Hertzian indentation method. Microstructural analysis indicated that for the three types of testing materials the contact damage was governed by multiple grain slip, crushed grains, and intergranular shear failure. No cone cracking or other macro-cracks were visible on or beneath the contact damage surfaces. Bending tests on the specimens containing single-cycle contact damage revealed that the resistance of $Ti_3Si(Al)C_2$ to strength degradation was significantly improved by incorporating SiC particles into the matrix. The mechanism of the improvement is ascribed to the increased shear resistance and the fact that the hard SiC particles inhibit the downward extent of the contact damage through restricting the slip and deformation of the $Ti_3Si(Al)C_2$ grains.

Keywords: $Ti_3Si(Al)C_2$-based materials; SiC; Strength; Surfaces

1. Introduction

The surfaces of structural ceramic components in service, such as contact bearings, extrusion modes, and turbine blades, are commonly subjected to concentrated loads. The stress from such contacts can introduce localized contact damage, which in turn can degrade the strength or erode the surface.[1–3] Depending on the contact loads, the retained strength may be governed by the pre-existing flaws or the "plastic deformation" induced by the contact damage. An important consideration in the stress concentrating applications is the retention of strength after the introduction of contact-related damage. From the viewpoints of service lifetime and safety design, it is interesting and necessary to study the resistance to strength degradation for the structural components. The layered ternary ceramic Ti_3SiC_2 is a promising structural material because of its unique combination of the merits of both metals and ceramics, such as low density, high elastic modulus, good oxidation resistance below 1100 °C, high flexural strength and fracture toughness, and good resistance to thermal shock.[4–9] However, few investigations on the resistance to strength degradation by contact loads for Ti_3SiC_2, to the best of our knowledge, can be found in the literature. El-Raghy et al.[10,11] measured the retained four-point flexural strength after the Vicker's indentations for the fine-grained and coarse-grained Ti_3SiC_2. Their results suggested that the resistance of Ti_3SiC_2 to strength degradation might be poor. Thus, there is a strong need to improve this resistance of Ti_3SiC_2 in order to widen its use in structural applications.

Ti_3SiC_2 has a hexagonal crystallographic structure with planar Si layers linked by TiC octahedrals. It has been demonstrated that Ti_3SiC_2 has a high Young's modulus ($E \approx 320$ GPa), but low hardness ($H_v \approx 4$ GPa).[4,6,9] The low H/E value indicates that this material is more reminiscent with soft metals and reveals a quasi-plasticity character. Lawn et al. pointed out that the subsurface damage responsible for the ductility originated from local shear-driven deformation processes,[12] as has been proven for a coarse-grain Ti_3SiC_2.[13] The subsurface damage in quasi-plastic ceramics like Ti_3SiC_2 must be induced by shear stresses, which in turn result in the strength degradation. Previous studies on the electronic structure of Ti_3SiC_2 disclosed

* Corresponding author at: Shenyang National Laboratory for Materials Science, Institute of Metal Research, Chinese Academy of Sciences, 72 Wenhua Road, Shenyang 110016, PR China. Tel.: +86 24 23971765; fax: +86 24 23891320.
E-mail address: yczhou@imr.ac.cn (Y. Zhou).

0955-2219/$ – see front matter © 2006 Elsevier Ltd. All rights reserved.
doi:10.1016/j.jeurceramsoc.2006.07.018

that the low shear resistance originated from the weak bonding between the Ti–C–Ti–C–Ti covalent bond chain and the Si layer, which resulted in a low shear modulus C_{44}.[14,15] Hence, the poor resistance to contact damage could be related to the low shear resistance in Ti_3SiC_2. It is known that incorporating hard particles, like SiC, can enhance the shear resistance, and thus the resistance to contact damage of the layered ceramics. Recently, $Ti_3Si(Al)C_2$/SiC composites have been prepared by in situ hot pressing/solid–liquid reaction process to improve the hardness, wear, and oxidation resistance of Ti_3SiC_2.[16] Despite many superior properties having been obtained, it is further expected that these $Ti_3Si(Al)C_2$/SiC composites would exhibit enhanced resistance to strength degradation.

To investigate the strength degradation resistance and to characterize damage accumulation of $Ti_3Si(Al)C_2$ and $Ti_3Si(Al)C_2$/SiC composites, spherical indentation tests (Hertzian test) were performed using various loads. The Hertzian test has proven to be a useful method for identifying and quantifying damage in ceramics.[17–19] In this paper, we investigate the contact deformations of $Ti_3Si(Al)C_2$-based materials and the relationship between the retained strength after single-cycle contact damage and Hertzian indentation loads. The results will be beneficial for the promotional application of $Ti_3Si(Al)C_2$ and $Ti_3Si(Al)C_2$/SiC composites as candidates for structural components and for understanding the effects of SiC on the resistance to strength degradation of $Ti_3Si(Al)C_2$-based materials.

2. Experimental procedure

Bulk $Ti_3Si(Al)C_2$, $Ti_3Si(Al)C_2$/10 vol.% SiC, and $Ti_3Si(Al)C_2$/30 vol.% SiC materials were fabricated by in situ hot pressing/solid–liquid reaction synthesis, which was also described elsewhere.[16] Briefly, the materials were made by the following procedure. Elemental powders, Ti, Si, Al, and graphite, were precisely weighed according to the target compositions and mixed for 15 h in a wet medium. After milling and drying, the mixtures were screened through a 60-mesh (about 221 μm) sieve and cold compacted into a Φ 50 mm graphite mold coated with boron nitride (BN). The green compacts were then hot pressed at 25 MPa in a flowing Ar atmosphere at 1550 °C for 60 min, and subsequently annealed at 1400 °C for 30 min. All of the as-prepared samples are fully dense (97–99% of the theoretical density). Table 1 shows the measured average grain size of the $Ti_3Si(Al)C_2$ and SiC particles in the composites. The typical properties of the $Ti_3Si(Al)C_2$, $Ti_3Si(Al)C_2$/10 vol.% SiC, and $Ti_3Si(Al)C_2$/30 vol.% SiC composites are listed in Table 2.

Specimens with a size of 3 mm × 4 mm × 36 mm were electrical-discharge machined from the bulk samples, and the surfaces of the specimens were ground and polished up to 1200# SiC grits. Hertzian contact tests were made on the polished surfaces of the testing samples to determine damage characteristics. In these tests, a tungsten carbide (WC) ball with a radius of 2 mm was used at various loads and the indents were made at the center of 4 mm × 36 mm surface of the samples. The loading speed was 0.5 kN/min and the holding time at the maximum load was 20 s. Acoustic emission (AE) counts were recorded during the loading, holding, and unloading processes of these Hertzian indentation tests.

Measurements of the contact radius, a, at each given load P and sphere radius, r, enabled calculation of the indentation stress, $P_0 = P/\pi a^2$, and the indentation strain, a/r, for the construction of an indentation stress–strain curve.[12,20] The degree of yield was determined from the indentation stress–strain curve as a deviation from Hertzian linear elastic response. The indent size was measured by optical microscopy (OM), and the tensile-fractured sections around the Hertzian indents were examined by means of scanning electron microscopy (SEM) (S-360, Cambridge Instruments Ltd., UK).

To investigate the subsurface indentation damage, sectional views of the damage patterns were obtained using bonded interface specimens.[12] These samples were prepared by bonding together two polished half-bars with a thin layer of adhesive, and then polishing the top surfaces. Hertzian indentations were made at the top surfaces symmetrically along the surface trace of the bonded interface. Finally, the adhesive was dissolved in ace-

Table 1
Measured average grain size of the $Ti_3Si(Al)C_2$ and SiC grains in the $Ti_3Si(Al)C_2$/SiC composites

Samples	$Ti_3Si(Al)C_2$		SiC	
	Grain length (μm)	Grain width (μm)	Grain length (μm)	Grain width (μm)
$Ti_3Si(Al)C_2$	16.1 ± 9.3	4.2 ± 1.4		
$Ti_3Si(Al)C_2$–10 vol.% SiC	12.8 ± 7.9	4.0 ± 1.8	16.2 ± 6.5	8.2 ± 3.1
$Ti_3Si(Al)C_2$–30 vol.% SiC	10.9 ± 4.7	4.1 ± 1.3	17.3 ± 7.2	8.6 ± 2.9

Table 2
Summary of the typical properties of the monolithic $Ti_3Si(Al)C_2$, $Ti_3Si(Al)C_2$/10 vol.% SiC, and $Ti_3Si(Al)C_2$/30 vol.% SiC

Properties	$Ti_3Si(Al)C_2$	$Ti_3Si(Al)C_2$/10 vol.% SiC	$Ti_3Si(Al)C_2$/30 vol.% SiC
Relative density (%)	98.7	98.2	97.5
Elastic modulus (GPa)	312	328	363
H_v (GPa)	4.02	6.99	12.70
Flexural strength (MPa)	418.8	356.9	339.4
Fracture toughness (MPa $m^{1/2}$)	6.24	6.49	6.97

tone, and the top and side surfaces of the separated half-blocks were examined by OM.

Retained strength tests were made on series of $Ti_3Si(Al)C_2$-based materials containing single-cycle contact damage to evaluate the degrading effect of the contact damage. Three-point bending tests were carried out at a crosshead speed of 0.5 mm/min on polished and chamfered bars with the indented surfaces on the tensile side. The contact damage was created by applying loads in the range of 0–1200 N. For each condition, three to five specimens were tested to ensure the veracity. After testing, the fracture surfaces of the samples with single-cycle contact damage were examined by means of SEM. Since $Ti_3Si(Al)C_2$-based materials are promising candidates for high temperature applications, the high-temperature retained strength of samples with single-cycle contact damage was also investigated.

To shed light on the mechanism for the effect of SiC on the strength degradation of $Ti_3Si(Al)C_2$-based materials, the shear strength was also measured. Samples for shear strength tests were thin slices with 20 mm × 30 mm in size and 0.1–0.2 mm in thickness. They were clamped between two square steel fixtures with through-holes that permitted the punch to pass through without friction. The shear strength was given as[21]:

$$\tau = \frac{P_C}{\pi dh}$$

where P_C is the critical load, d is the punch diameter, and h is the thickness of the samples. The cross-section micrographs of the punched disks were also examined via SEM.

3. Results

3.1. Indentation stress–strain curves

The indentation stress–strain curves (Fig. 1) for the materials with different compositions deviate distinctly from linearity at high stress. The yield stress is highest for the $Ti_3Si(Al)C_2$/30 vol.% SiC composite, and lowest for monolithic $Ti_3Si(Al)C_2$, consistent with the apparent tendency of increasing hardness with increasing SiC content in the composites. The critical indentation stress (at yield) is about 2.5 GPa, 4.0 GPa, and 5.8 GPa for $Ti_3Si(Al)C_2$, $Ti_3Si(Al)C_2$/10 vol.% SiC, and $Ti_3Si(Al)C_2$/30 vol.% SiC composite, respectively. Fischer-Cripps et al.[22] showed many typical indentation stress–strain curves of quasi-plastic materials including steel, glass–ceramic, silicon nitride, and tungsten carbide (soft → hard). Compared with those curves, it was found that the character of $Ti_3Si(Al)C_2$ was very similar to that of steel, while the behaviors of the composites resembled that of glass–ceramic. These results demonstrate that $Ti_3Si(Al)C_2$-based materials belong to the class of quasi-plastic materials, and the critical indentation stress is increased with increasing SiC contents due to the contribution of the hard SiC particles.

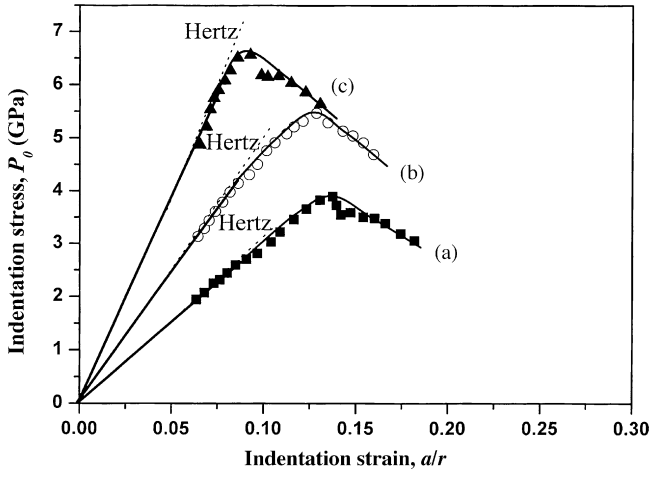

Fig. 1. Hertzian indentation stress–strain curves for monolithic $Ti_3Si(Al)C_2$ (a), $Ti_3Si(Al)C_2$/10 vol.% SiC (b) and $Ti_3Si(Al)C_2$/30 vol.% SiC (c) composites. Data points are taken from experiments using a tungsten carbide sphere with a radius of 2 mm. Inclined dashed line is Hertzian elastic response.

Fig. 2(a–c) compare the surface views of the retained contact sites on each of the $Ti_3Si(Al)C_2$-based materials after loading to 1000 N, along with corresponding acoustic signal traces over the full loading–holding–unloading cycle. For each material, an obvious plastic spherical indent is found, and no indentation induced cracks are found around the indent. At the given load, the indent size decreases with increasing SiC content, which is in agreement with the fact that the hardness of $Ti_3Si(Al)C_2$ is greatly enhanced by incorporating SiC particles.[16] It is also found that the corresponding acoustic signatures are very weak (the maximum intensity is less than 55), suggesting that no obvious cracks were formed during the whole testing process. With increasing SiC content, the acoustic signals from the $Ti_3Si(Al)C_2$/SiC composites decrease, but the maximum intensity increases. It is demonstrated that $Ti_3Si(Al)C_2$-based materials become hardened with the increment of SiC content, which is in agreement with the results shown in Fig. 1.

3.2. Retained strength tests

Fig. 3(a) shows the relationship between the retained flexural strength and Hertzian indentation loads. The retained flexural strength of $Ti_3Si(Al)C_2$ remains roughly constant up to a load of 250 N, and then decreases rapidly when the load is beyond this value, which indicates that the critical indentation load controlling the fracture is about 250 N. For the composites containing 10 vol.% SiC and 30 vol.% SiC, the critical loads are about 400 N and 1000 N, respectively. The retained strengths fluctuate within a narrow range and are quite close to the initial strength as a result of natural flaws before the critical indentation load. Beyond the critical indentation load, the retained strength decreases rapidly with increasing indentation load. The flaws induced by contact damage should have controlled the measured strengths and resulted in the strength degradation. In another word, the deleterious effect of the indentation loads could be neglected when the applied loads are lower than the critical indentation load. Fig. 3(b) represents the retained flexural strength as a function of Hertzian indentation size. The corresponding critical indentation size (2a) for $Ti_3Si(Al)C_2$, $Ti_3Si(Al)C_2$/10 vol.% SiC, and $Ti_3Si(Al)C_2$/30 vol.% SiC composites are 350 μm, 372 μm, and 498 μm, respectively. Both the critical indentation load and the

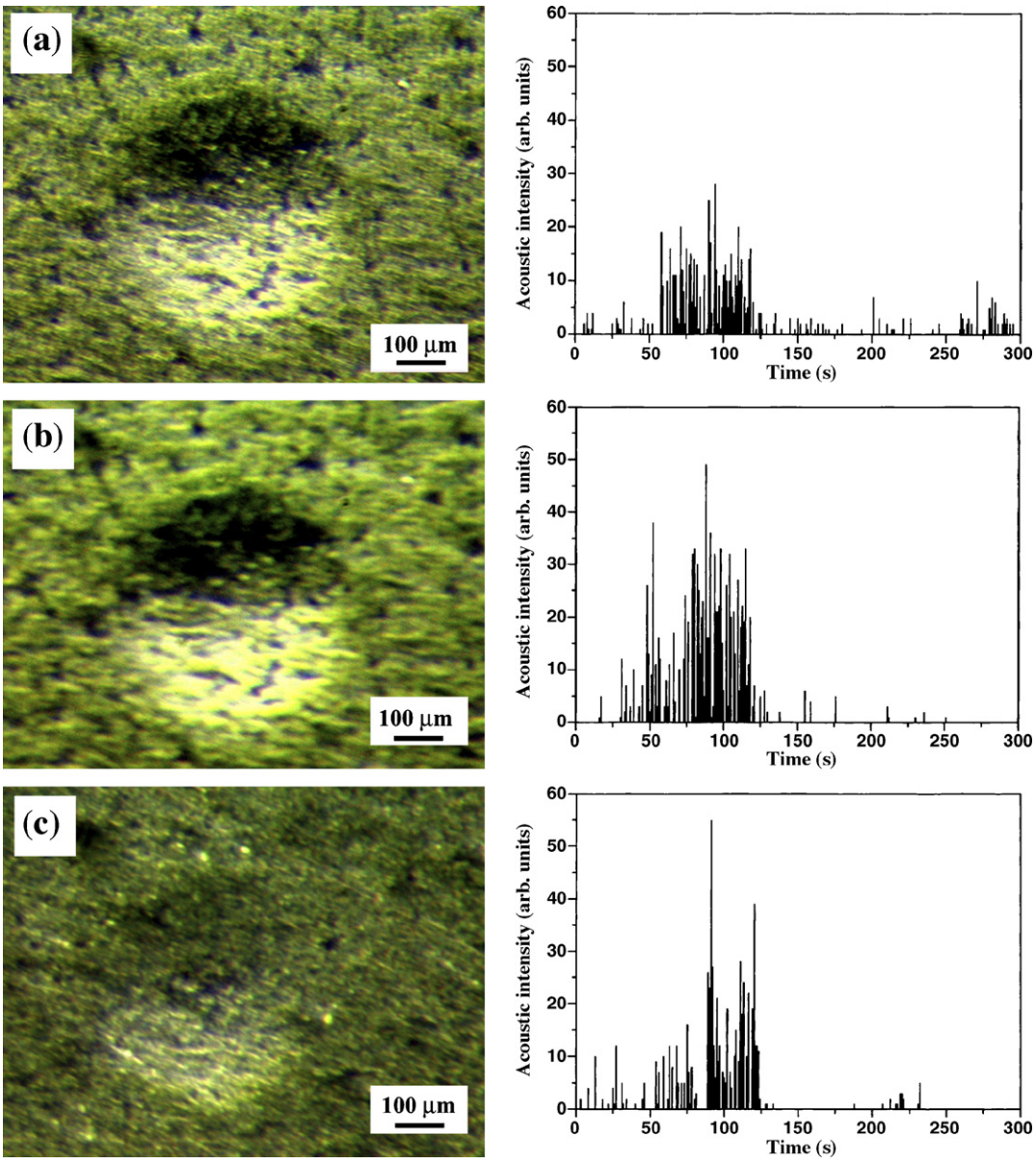

Fig. 2. Hertzian contact sites in $Ti_3Si(Al)C_2$ (a), $Ti_3Si(Al)C_2$/10 vol.% SiC (b), and $Ti_3Si(Al)C_2$/30 vol.% SiC (c) materials caused by loading a WC sphere with a radius of 2 mm to 1000 N. Left column: optical micrographs showing surface views. Right column: the corresponding acoustic emission signals for the full loading–holding–unloading process.

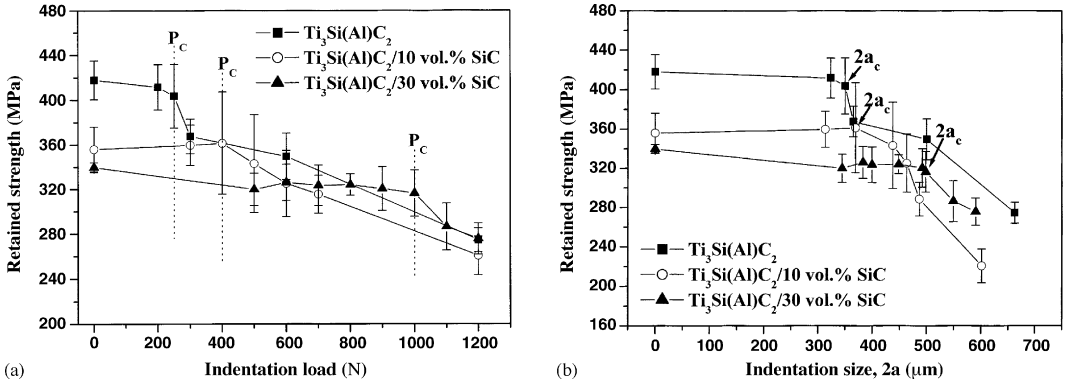

Fig. 3. (a) Strength degradation for $Ti_3Si(Al)C_2$, $Ti_3Si(Al)C_2$/10 vol.% SiC, and $Ti_3Si(Al)C_2$/30 vol.% SiC materials due to the contact damage made by a WC sphere, $r = 2$ mm. Vertical dashed lines indicate the critical loads for the onset of strength-degrading damage. (b) The retained strength of $Ti_3Si(Al)C_2$, $Ti_3Si(Al)C_2$/10 vol.% SiC, and $Ti_3Si(Al)C_2$/30 vol.% SiC materials as a function of the Hertzian indentation sizes corresponding to the applied loads.

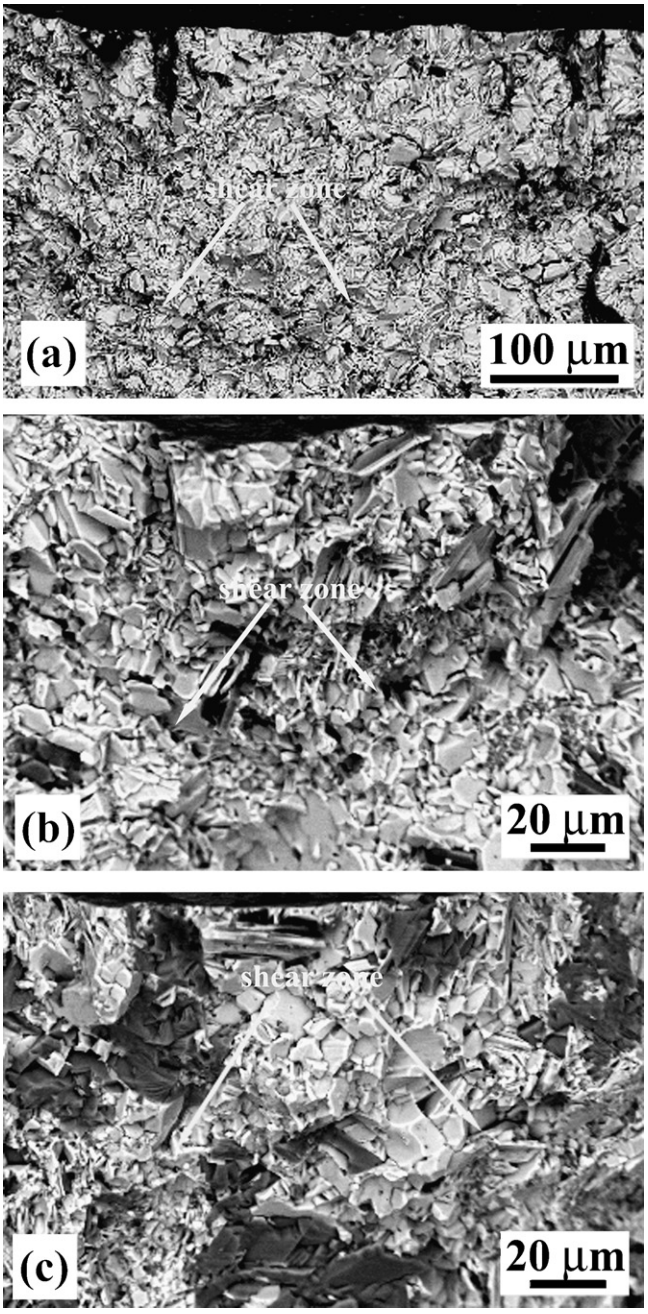

Fig. 4. SEM backscattered electron images of the fracture surfaces of the $Ti_3Si(Al)C_2$ (a), $Ti_3Si(Al)C_2$/10 vol.% SiC (b), and $Ti_3Si(Al)C_2$/30 vol.% SiC (c) materials with contact damage after bending tests. The contact damage was made at a fixed load of 1200 N for all three materials.

critical indentation size are increased with increasing SiC content. It is demonstrated that the resistance of $Ti_3Si(Al)C_2$ to strength degradation after single-cycle contact damage is greatly enhanced.

Fig. 4 compares the characteristic fracture surfaces of $Ti_3Si(Al)C_2$ (Fig. 4a), $Ti_3Si(Al)C_2$/10 vol.% SiC (Fig. 4b), and $Ti_3Si(Al)C_2$/30 vol.% SiC (Fig. 4c) composites with contact damage made at a load of 1200 N after bending tests. For each material, the damage zones are made up of multiple grain slip, crushed grains, and intergranular shear failure. The Hertzian indent zone is the largest for $Ti_3Si(Al)C_2$ and the smallest for

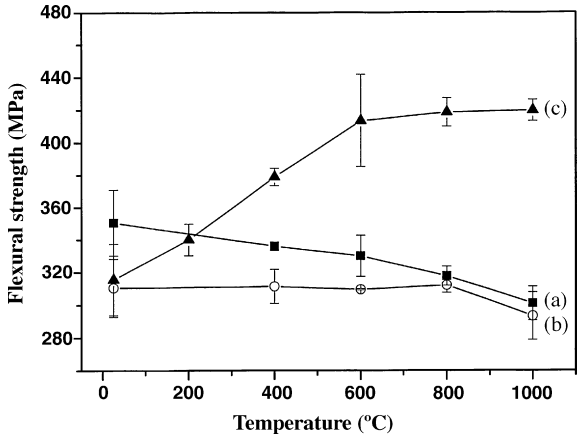

Fig. 5. Flexural strength of the $Ti_3Si(Al)C_2$ (a), $Ti_3Si(Al)C_2$/10 vol.% SiC (b), and $Ti_3Si(Al)C_2$/30 vol.% SiC (c) materials with the same indentation size (498 ± 7 μm) as a function of testing temperatures.

the $Ti_3Si(Al)C_2$/30 vol.% SiC composite. No cone cracks or other macro-cracks occur around the Hertzian indents, which is attributed to the good damage tolerance shown in previous works.[4,8,9,16]

The flexural strength of the $Ti_3Si(Al)C_2$/SiC composites with the same single-cycle contact damage size (498 ± 7 μm) at room temperature to high temperatures up to 1000 °C are presented in Fig. 5 and compared with that of monolithic $Ti_3Si(Al)C_2$. The applied loads to induce the same indentation size were 600 N for $Ti_3Si(Al)C_2$, 720 N for $Ti_3Si(Al)C_2$/10 vol.% SiC, and 1000 N for the $Ti_3Si(Al)C_2$/30 vol.% SiC composite. It can be seen that the retained strengths for $Ti_3Si(Al)C_2$ and the $Ti_3Si(Al)C_2$/10 vol.% SiC composite almost remain constant for all of the testing temperatures. Since the applied loads are higher than the critical indentation loads (250 N for $Ti_3Si(Al)C_2$ and 400 N for the $Ti_3Si(Al)C_2$/10 vol.% SiC composite), the induced flaws should govern the retained strength. Hence, it is not unreasonable to believe that the strength of testing specimens with contact damage is insensitive to the temperature. For the $Ti_3Si(Al)C_2$/30 vol.% SiC composite, the retained strengths at temperatures above 600 °C are higher than those of monolithic $Ti_3Si(Al)C_2$. At 1000 °C, the retained strength of the $Ti_3Si(Al)C_2$/30 vol.% SiC composite is about 415 MPa, which is about 40% higher than that of monolithic $Ti_3Si(Al)C_2$ at the same temperature. It can also be seen that the retained strength of $Ti_3Si(Al)C_2$/30 vol.% SiC composite increases with increasing temperature from room temperature to 600 °C, and then remains essentially constant when the temperatures further increase up to 1000 °C. A similar trend and practically the same strength for the $Ti_3Si(Al)C_2$/30 vol.% SiC composite without contact damage have been reported in our previous work.[23] A possible mechanism for this improvement of the high-temperature strength was also proposed. Because the applied load to induce contact damage (1000 N) is the same as the critical indentation load controlling the fracture, the retained strength should be governed by the natural flaws and the residual stress distribution in the specimens, viz. the induced contact damage at 1000 N will have little effect on the high-temperature retained strength for the $Ti_3Si(Al)C_2$/30 vol.% SiC composite.

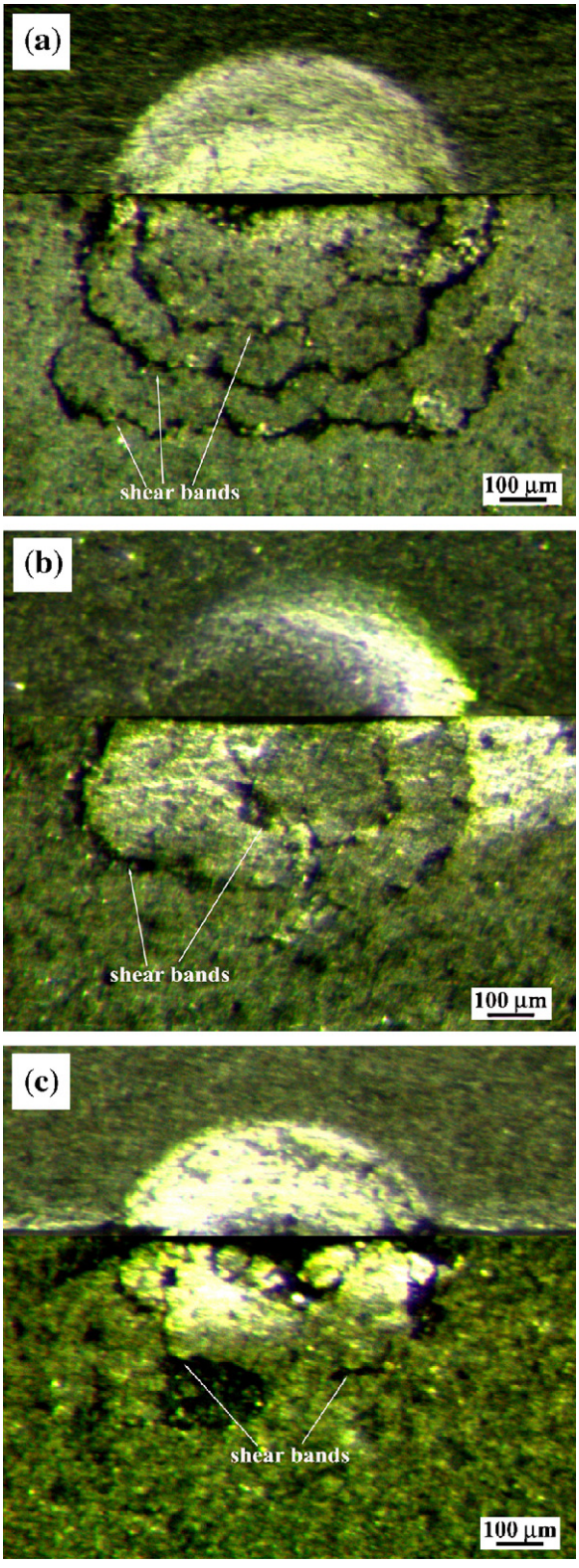

Fig. 6. OM micrographs showing half-surface and sectional views of indentation sites in $Ti_3Si(Al)C_2$ (a), $Ti_3Si(Al)C_2$/10 vol.% SiC (b), and $Ti_3Si(Al)C_2$/30 vol.% SiC (c) materials. The indentations were made at a fixed indentation load of 1200 N using a WC sphere with a radius of 2 mm.

3.3. Observation of contact damage zones

Fig. 6 compares the half surface (upper) and bonded interface cross-sectional views (lower) of contact damage formed at a relatively high load ($P = 1200$ N) for the monolithic $Ti_3Si(Al)C_2$ (Fig. 6a), $Ti_3Si(Al)C_2$/10 vol.% SiC (Fig. 6b), and $Ti_3Si(Al)C_2$/30 vol.% SiC (Fig. 6c), respectively. In the top views there are no cracks visible but obvious pileups are found around the indents. The size of the contact zone decreased with increasing SiC content in the composites due to the increased hardness. In the cross-sectional views the plastic zone extends downward and outward well beyond the contact on a near-hemispherical front. A number of apparent shear-bands are also found for $Ti_3Si(Al)C_2$, which confirms that the shear-activated basal slip deformation within and between grains is responsible for the high quasi-plasticity.[13] With increasing SiC content, the amount of shear-bands is reduced and the plastic deformation (mainly the shear zone) is not serious, viz. the resistance to surface damage is enhanced with the increase of SiC content in the composites.

3.4. Shear strength tests

To better understand the mechanism for the improvement, the punch–shear method[21] was introduced, which has been demonstrated to be a simple and feasible method for determining the shear strength of layered ceramics.[24] Changes of the measured shear strengths of $Ti_3Si(Al)C_2$-based materials are shown in Fig. 7. The shear strengths of $Ti_3Si(Al)C_2$, $Ti_3Si(Al)C_2$/10 vol.% SiC, and $Ti_3Si(Al)C_2$/30 vol.% SiC materials are 116.3 ± 9.4 GPa, 137.8 ± 7.6 GPa, and 177.1 ± 4.9 GPa, respectively. These results demonstrate that the shear strength of $Ti_3Si(Al)C_2$ is remarkably enhanced by adding hard SiC particles into the matrix. The cross-section micrographs of the punch disks are shown in Fig. 8. For $Ti_3Si(Al)C_2$ (Fig. 8a), comminuted grains of $Ti_3Si(Al)C_2$ are distributed in the friction area, while delamination, grain-buckle, intergranular, and transgranular fractures are observed in the unfriction region. On the other hand, for the $Ti_3Si(Al)C_2$/10 vol.% SiC (Fig. 8b) and $Ti_3Si(Al)C_2$/30 vol.%

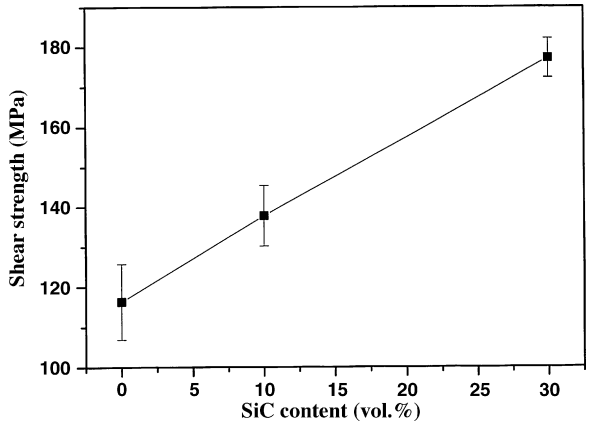

Fig. 7. Measured shear strengths vs. SiC contents for $Ti_3Si(Al)C_2$-based materials.

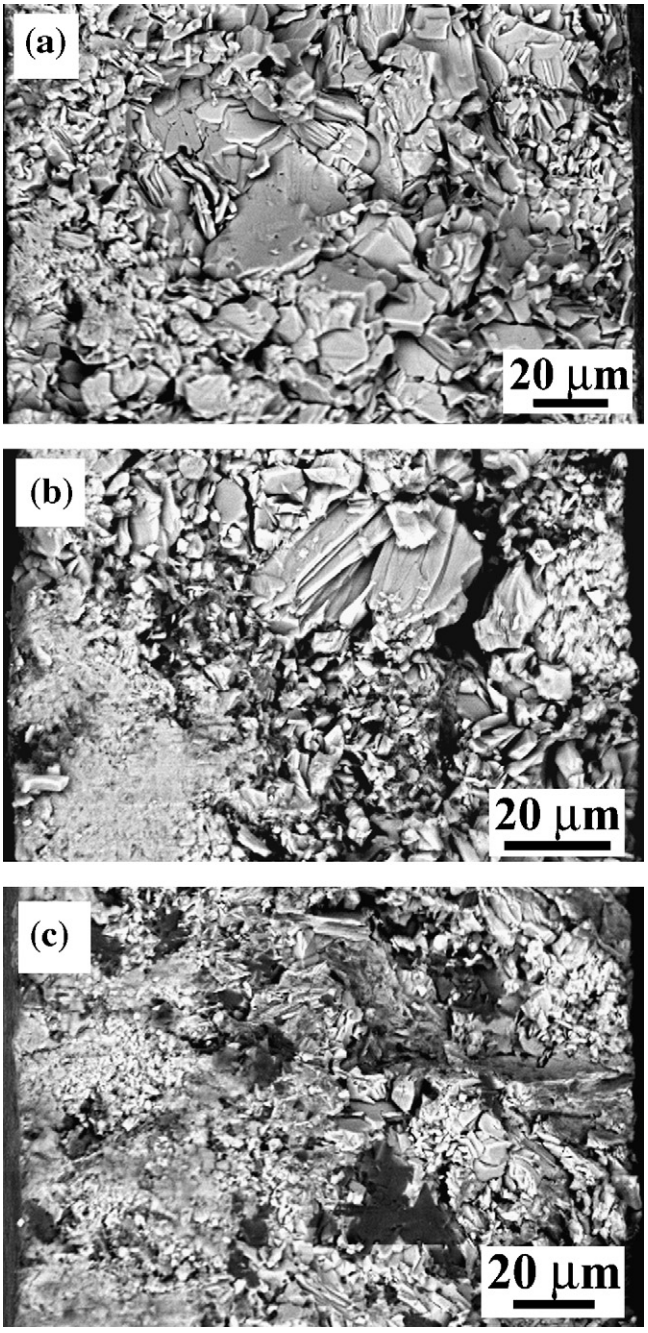

Fig. 8. Cross-section micrographs of the punch disks for $Ti_3Si(Al)C_2$ (a), $Ti_3Si(Al)C_2$/10 vol.% SiC (b), and $Ti_3Si(Al)C_2$/30 vol.% SiC (c) materials.

SiC composites (Fig. 8c), the SiC particles inhibit the fracture through restricting the slip and deformation of $Ti_3Si(Al)C_2$ grains. The $Ti_3Si(Al)C_2$/SiC composites show superior shear strength because of the contribution of the SiC particles, and the shear resistance will become stronger with the increase of SiC content.

4. Discussion

Our experiments confirm that shear-activated basal slip deformation within and between grains resulting in shear bands is the key factor for the exceptional high quasi-plasticity, which is in good agreement with previous works.[13,25] The most important result of this work is that the resistance of $Ti_3Si(Al)C_2$ to strength-impairing contact damage is greatly enhanced by the addition of SiC. As mentioned in Section 1, the improvement in the resistance to contact damage is related to the enhanced shear resistance. Due to the increased shear resistance, the obvious shear bands and the contact damage area become less with increasing SiC content in the composites at the same indentation loads (Figs. 4 and 6), and the critical indentation load to induce strength degradation is increased (Fig. 3a).

Although $Ti_3Si(Al)C_2$-based materials become harder and more brittle with the increase of SiC content,[16] the threshold of indentation size to induce the strength degradation is increased, which is uncommon for quasi-plastic materials. This apparent paradox needs to be investigated by consideration of the effect of SiC on the microstructures and can be explained according to the following facts. First, it is clear that the maximum depth of the shear zone is greatly reduced with the increase of SiC content at the same applied load (Fig. 6). Second, the downward extent of the contact damage zone in the sectional views becomes less with the increase of SiC content if the indentation sizes on the surface are the same (not shown here). Finally, the indentation size measured from the top views of the samples may not reflect the true contact damage. The shear zones in the sectional views should predominately influence on the measured retained strength by three-point bending tests for the specimens containing single-cycle contact damage. Under these conditions, since the hard SiC particles will restrict the downward extension of plastic deformation (mainly the shear bands) of the $Ti_3Si(Al)C_2$ matrix, the critical indentation size to induce strength degradation increases with the increment of SiC content. Therefore, the mechanism for the improvement of strength degradation resistance of $Ti_3Si(Al)C_2$ with single-cycle contact damage by incorporating SiC particles, is ascribed to the increased shear resistance and the fact that hard SiC particles inhibit the downward extent of the contact damage through restricting the slip and deformation of $Ti_3Si(Al)C_2$ grains.

5. Conclusions

The resistance of $Ti_3Si(Al)C_2$ to strength-impairing contact damage was significantly enhanced by incorporating SiC particles into the matrix. Bending tests on the samples containing single-cycle contact damage indicate that both the critical indentation load and the critical indentation size are increased with the increase of SiC contents. The $Ti_3Si(Al)C_2$/30 vol.% SiC composite shows a critical indentation load of 1000 N to induce strength degradation, which is three times higher than that of monolithic $Ti_3Si(Al)C_2$. The corresponding critical indentation size of the $Ti_3Si(Al)C_2$/30 vol.% SiC composite is about 498 μm, which is 42.3% higher than that of $Ti_3Si(Al)C_2$. The enhanced resistance to strength degradation is due to the increased shear strength and the fact that the hard SiC particles inhibit the downward extent of the contact damage through restricting the slip and deformation of $Ti_3Si(Al)C_2$ grains.

Acknowledgements

This work was supported by the National Outstanding Young Scientist Foundation (no. 59925208 for Y.C. Zhou, no. 50125204 for Y.W. Bao), Natural Sciences Foundation of China under Grant no. 50232040, no. 50302011, no. 90403027, '863' project, "Hundred talent-plan", High-tech Bureau of the Chinese Academy of Sciences, and French Atomic Energy Commission (CEA).

References

1. Wiederhorn, S. M. and Lawn, B. R., Strength degradation of glass resulting from impact with spheres. *J. Am. Ceram. Soc.*, 1977, **60**(9–10), 451–458.
2. Lawn, B. R., Wiederhorn, S. M. and Johnson, H. H., Strength degradation of brittle surfaces: blunt indenters. *J. Am. Ceram. Soc.*, 1975, **58**(9–10), 428–432.
3. Wiederhorn, S. M. and Hockey, B. J., Effect of material parameters on the erosion resistance of brittle materials. *J. Mater. Sci.*, 1983, **18**, 766–780.
4. Barsoum, M. W. and El-Raghy, T., Synthesis and characterization of a remarkable ceramic: Ti_3SiC_2. *J. Am. Ceram. Soc.*, 1996, **79**, 1953–1956.
5. Zhou, Y. C., Sun, Z. M., Sun, J., Zhang, Y. and Zhou, J., Titanium silicon carbide: a ceramic or a metal? *Z. Metallkd.*, 2000, **91**, 329–334.
6. Barsoum, M. W., The $M_{N+1}AX_N$ phases: a new class of solids; thermodynamically stable nanolaminates. *Prog. Solid. Chem.*, 2000, **28**, 201–281.
7. Sun, Z. M., Zhou, Y. C. and Li, M. S., High temperature oxidation behavior of Ti_3SiC_2-based material in air. *Acta Mater.*, 2001, **49**(20), 4347–4353.
8. Low, I. M., Vickers contact damage of micro-layered Ti_3SiC_2. *J. Eur. Ceram. Soc.*, 1998, **18**, 709–713.
9. Zhou, Y. C., Sun, Z. M. and Yu, B. H., Microstructure of Ti_3SiC_2 prepared by the in-situ hot pressing/solid–liquid reaction process. *Z. Metallkd.*, 2000, **91**(11), 937–941.
10. El-Raghy, T., Zavaliangos, A., Barsoum, M. W. and Kalidindi, S. R., Damage mechanism around hardness indentation in Ti_3SiC_2. *J. Am. Ceram. Soc.*, 1997, **80**(2), 513–516.
11. El-Raghy, T., Barsoum, M. W., Zavaliangos, A. and Kalidindi, S. R., Processing and mechanical properties in Ti_3SiC_2. II. Effect of grain size and deformation temperature. *J. Am. Ceram. Soc.*, 1999, **82**(10), 2855–2860.
12. Lawn, B. R., Padture, N. P., Cai, H. and Guiberteau, F., Making ceramics "Ductile". *Science*, 1994, **263**, 1114–1116.
13. Low, I. M., Lee, S. K. and Lawn, B. R., Contact damage accumulation in Ti_3SiC_2. *J. Am. Ceram. Soc.*, 1998, **81**, 225–228.
14. Zhou, Y. C. and Sun, Z. M., Electronic structure and bonding properties in layered ternary carbide Ti_3SiC_2. *J. Phys. Condens. Mater.*, 2000, **12**(28), L457–L462.
15. Wang, J. Y. and Zhou, Y. C., Polymorphism of Ti_3SiC_2 ceramic: first-principle investigations. *Phys. Rev. B.*, 2004, **69**, 144108.
16. Wan, D.T., Zhou, Y.C., Bao, Y.W. and Yan, C. K., In-situ reaction synthesis and characterization of $Ti_3Si(Al)C_2$/SiC composites. *Ceram. Int.*, in press [Corrected proof available on line].
17. Cai, H., Kalceff, M. A. and Lawn, B. R., Deformation and fracture of mica-containing glass–ceramics in Hertzian Contacts. *J. Mater. Res.*, 1994, **9**(3), 762–770.
18. Pajares, A., Guiberteau, F., Lawn, B. R. and Lathabai, S., Hertzian contact damage in magnesia-partially-stabilized zirconia. *J. Am. Ceram. Soc.*, 1995, **78**(4), 1083–1086.
19. Guiberteau, F., Padture, N. P. and Lawn, B. R., Effect of grain size on Hertzian contact damage in alumina. *J. Am. Ceram. Soc.*, 1994, **77**(7), 1825–1831.
20. Lawn, B. R., Indentation of ceramics with spheres: a century after Hertz. *J. Am. Ceram. Soc.*, 1998, **81**(8), 1977–1994.
21. Bao, Y. W., Zhang, H. B. and Zhou, Y. C., Punch–shear tests and size effects for evaluating the shear strength of machinable ceramics. *Z. Metallkd.*, 2004, **95**, 372–376.
22. Fischer-Cripps, A. C. and Lawn, B. R., Stress analysis of contact deformation in quasi-plastic ceramics. *J. Am. Ceram. Soc.*, 1996, **79**(10), 2609–2618.
23. Zhou, Y. C., Wan, D. T., Bao, Y. W. and Wang, J. Y., In-situ processing and high-temperature properties of $Ti_3Si(Al)C_2$/SiC composites. *Int. J. Appl. Ceram. Technol.*, 2006, **3**(1), 47–54.
24. Bao, Y. W., Chen, J. X., Wang, X. H. and Zhou, Y. C., Shear strength and shear failure of layered machinable Ti_3AlC_2 ceramics. *J. Eur. Ceram. Soc.*, 2004, **24**, 855–860.
25. Zhou, Y. C. and Sun, Z. M., Microstructure and mechanism of damage tolerance for Ti_3SiC_2 bulk ceramics. *Mater. Res. Innovat.*, 1999, **2**, 360–363.